



Published in final edited form as:

Cell Rep. 2018 January 02; 22(1): 189–205. doi:10.1016/j.celrep.2017.12.038.

Primary Cilium-Mediated Retinal Pigment Epithelium Maturation Is Disrupted in Ciliopathy Patient Cells

Helen Louise May-Simera^{1,7}, Qin Wan^{2,7}, Balendu Shekhar Jha^{2,7}, Juliet Hartford², Vladimir Khristov², Roba Dejene², Justin Chang², Sarita Patnaik¹, Quanlong Lu³, Poulomi Banerjee⁴, Jason Silver², Christine Insinna-Kettenhofen³, Dishita Patel², Mostafa Lotfi², May Malicdan⁶, Nathan Hotaling², Arvydas Maminishkis², Rupa Sridharan⁵, Brian Brooks², Kiyoharu Miyagishima², Meral Gunay-Aygun⁶, Rajarshi Pal⁴, Christopher Westlake³, Sheldon Miller², Ruchi Sharma², and Kapil Bharti^{2,8,*}

¹Institute of Molecular Physiology, Johannes-Gutenberg University, Mainz, Germany

²National Eye Institute, NIH, Bethesda, MD, USA

³National Cancer Institute, NIH, Frederick, MD, USA

⁴School of Regenerative Medicine, Manipal University, Bangalore, India

⁵University of Wisconsin, Madison, WI, USA

⁶National Human Genome Research Institute, NIH, Bethesda, MD, USA

⁷These authors contributed equally

⁸Lead Contact

SUMMARY

Primary cilia are sensory organelles that protrude from the cell membrane. Defects in the primary cilium cause ciliopathy disorders, with retinal degeneration as a prominent phenotype. Here, we demonstrate that the retinal pigment epithelium (RPE), essential for photoreceptor development and function, requires a functional primary cilium for complete maturation and that RPE maturation defects in ciliopathies precede photoreceptor degeneration. Pharmacologically enhanced ciliogenesis in wild-type induced pluripotent stem cells (iPSC)-RPE leads to fully mature and functional cells. In contrast, ciliopathy patient-derived iPSC-RPE and iPSC-RPE with a knockdown of ciliary-trafficking protein remain immature, with defective apical processes, reduced functionality, and reduced adult-specific gene expression. Proteins of the primary cilium

This is an open access article under the CC BY-NC-ND license (<http://creativecommons.org/licenses/by-nc-nd/4.0/>).

*Correspondence: kapilbharti@mail.nih.gov.

AUTHOR CONTRIBUTIONS

H.L.M.-S. and K.B. were responsible for conception and experimental design. H.L.M.-S., Q.W., B.S.J., J.H., V.K., R.D., J.C., S.P., Q.L., P.B., J.S., C.I.-K., D.P., M.L., M.M., N.H., A.M., R. Sridharan, K.M., and R. Sharma performed experiments. N.H. and K.M. performed analyses. B.B., M.G.-A., C.W., and S.M. provided reagents. H.L.M.-S., Q.W., and K.B. generated figures. H.L.M.-S., Q.W., and K.B. co-wrote the manuscript.

SUPPLEMENTAL INFORMATION

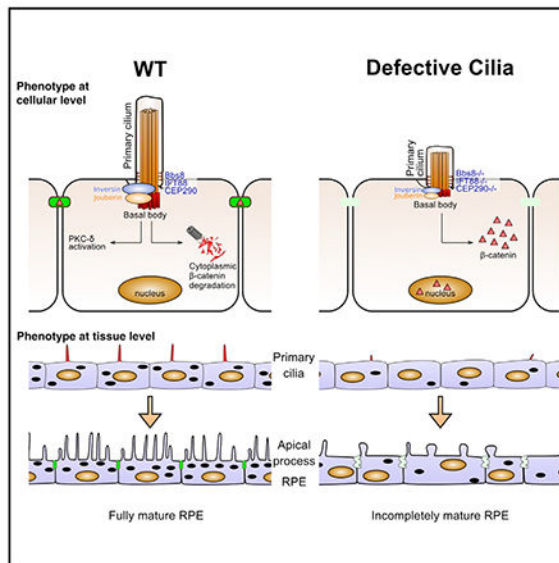
Supplemental Information includes Supplemental Experimental Procedures, six figures, and four tables and can be found with this article online at <https://doi.org/10.1016/j.celrep.2017.12.038>.

DECLARATION OF INTERESTS

The authors declare no competing interests.

regulate RPE maturation by simultaneously suppressing canonical WNT and activating PKC δ pathways. A similar cilium-dependent maturation pathway exists in lung epithelium. Our results provide insights into ciliopathy-induced retinal degeneration, demonstrate a developmental role for primary cilia in epithelial maturation, and provide a method to mature iPSC epithelial cells for clinical applications.

Graphical Abstract



In Brief

May-Simera et al. show that primary cilia regulate the maturation and polarization of human iPSC-RPE, mouse RPE, and human iPSC-lung epithelium through canonical WNT suppression and PKC δ activation. RPE cells derived from ciliopathy patients exhibit defective structure and function. These results provide insights into ciliopathy-induced retinal degeneration.

INTRODUCTION

Primary cilia are microtubule-based appendages that extend from the cell membrane and are required for a variety of cellular processes. Since their initial discovery in the 18th century (Dobell, 1932; Muller, 1786), primary cilia have been identified on most eukaryotic cell types during some phase of their development (Gerdes et al., 2009). Primary cilia are anchored to the cell via a basal body derived from the mother centriole. In contrast to motile cilia, in which the extra central pair of microtubules is required for generation of movement, primary cilia are composed only of nine microtubule doublets extending from microtubule triplets of the basal body (Reiter et al., 2012). Although the precise composition of ciliary membrane proteins and inventory of signaling molecules differs between cell type and cell stage, primary cilia have been shown to act as a sensory signaling hub, regulating ubiquitous developmental pathways such as Sonic Hedgehog (SHH), transforming growth factor β (TGF- β), and WNT (May-Simera and Kelley, 2012b; Sasai and Briscoe, 2012). Moreover,

ciliogenesis per se is highly regulated by extra-cellular and intracellular signaling (Kim and Dynlacht, 2013).

In the vertebrate eye, in addition to the retinal photoreceptors that contain a highly modified primary cilium, primary cilia are present in numerous different cell types, including the cornea, the trabecular meshwork, the lens, and the retinal pigment epithelium (RPE) (Grisanti et al., 2016; Luo et al., 2012; May-Simera et al., 2017; Sugiyama et al., 2010). The RPE is a polarized epithelial tissue located in the back of the eye (Bharti et al., 2011), and a vast majority of *in vitro* cilium studies utilize immortalized RPE cell lines such as ARPE19 and hTERT-RPE-1. However, not much is known about the function of primary cilia *in vivo* in mouse or human RPE. In other epithelial tissues, such as the organ of Corti in the cochlea, the primary cilium is associated with the formation of actin-based stereocilia on the apical surface, complete tissue maturation, and functionality (Denman-Johnson and Forge, 1999; May-Simera and Kelley, 2012a). Similar actin-based apical processes extend from the apical surface of RPE cells and are a hallmark of RPE polarization and function (Lehmann et al., 2014).

Defects in primary cilium function cause a spectrum of human diseases collectively termed ciliopathies (Braun and Hildebrandt, 2017). Ciliopathies have overlapping clinical phenotypes and were originally categorized based on subtle phenotypic differences (Lee and Gleason, 2011). Retinal degeneration is the most frequent phenotype present across most ciliopathy patients (Bujakowska et al., 2017; Wheway et al., 2014). Retinal degeneration is predominantly thought to be caused by functional and developmental abnormalities in retinal photoreceptors such that their outer segments do not fully develop and undergo rapid degeneration. However, the contribution of defective cilia from non-photoreceptor ocular cell types to the retinal degeneration seen in ciliopathy patients has not been investigated. Previous work suggests that photoreceptor outer segment development is dependent on complete maturation of the RPE monolayer located adjacent to the retinal photoreceptors (Nasonkin et al., 2013). Furthermore, it has also long been established that photoreceptor health and functional integrity are critically dependent on functional and metabolic support from RPE cells that tightly associate with retinal photoreceptors anatomically (Bharti et al., 2011). It is not clear whether defective cilia in the RPE may contribute to initiation and/or progression of retinal degeneration in patients.

The pleiotropic role of the primary cilium across multiple tissues is principally due to its ability to modulate various signaling pathways. One of the first signaling pathways shown to be associated with the primary cilium function is the WNT signaling pathway (May-Simera and Kelley, 2012b). The canonical branch of WNT signaling leads to the stabilization of cytoplasmic β -catenin, which translocates into the nucleus, where it activates transcription of target genes. β -catenin activity has been shown to be suppressed by the cilium via sequestration of its activator JOUBERIN (Ahi1) to the cilium base (Lancaster et al., 2011). Regulation of WNT signaling is critical for RPE development (Westenskow et al., 2009). Another key cellular process controlled by the primary cilium in epithelial cells, via the regulation of non-canonical WNT signaling, is the planar cell polarity, which results in functional polarization across an epithelial plane (May-Simera et al., 2015; Ross et al., 2005

Roignot et al., 2013). This is a key step in RPE maturity and functionality, but the role of primary cilia in this process is not fully understood.

Based on literature and our current data (Figures 1A–1D) regarding the presence of primary cilia in confluent monolayers of human and mouse RPE, we examined the function of this organelle in the RPE (Parfitt et al., 2016). Experimentally enhanced ciliogenesis using specific drugs led to improved maturation and functionality in human induced pluripotent stem cell (hiPSC)-RPE, whereas inhibition of the primary cilium function led to incompletely matured induced pluripotent stem cell (iPSC)-RPE cells. Downstream of the cilium, this effect is mediated by canonical WNT suppression, leading to cell cycle exit in iPSC-RPE and protein kinase C δ (PKC δ) activation, likely initiated by direct protein-protein interactions between the cilium trafficking protein BBS8 and canonical WNT effectors INVERSIN and JOUBERIN. The effect of enhanced ciliogenesis on epithelial maturation can be generalized to at least one more epithelial cell type: the iPSC-proximal lung epithelial cells. Furthermore, genetic knockdown of the cilium gene IFT88 confirmed that primary cilia regulate complete maturation and apical-basal polarization of the RPE. To confirm these findings obtained with pharmacological modulation of primary cilia, we used RPE cells derived from a ciliopathy patient and a ciliopathy mouse model. These two independent models confirmed a major role for the RPE in the retinal degeneration phenotype seen in ciliopathy patients: iPSC-RPE derived from a ciliopathy (Joubert syndrome) patient with CEP290 mutations demonstrated a lack of structural and functional maturity; *Bbs8*^{-/-} mice with abnormal cilia revealed that the RPE maturation defect precedes photoreceptor maturation. This work has helped to develop mature and polarized iPSC-RPE for autologous cell therapy of age-related macular degeneration (AMD) patients and also highlights the need for considering the RPE as well when developing treatment strategies for retinal degeneration in ciliopathy patients.

RESULTS

Primary Cilium Induction Helps Generate Fully Mature and Functional hiPSC-Derived RPE

The emergence of primary cilia on hiPSC-RPE cells (Figure 1B) and mouse RPE (Figures 1C and 1D) temporally coincides with the maturation of cells and precedes induction of apical processes. iPSC-derived RPE cells formed primary cilia, as confirmed by ARL13B and GT335 immunostaining (Figure 1E), but ciliogenesis was not seen in all cells across the monolayer. Furthermore, RPE cells derived from iPSCs do not fully mature *in vitro* (Figures 1I and 1M). Based on these observations, we hypothesized that primary cilia regulate complete maturation of RPE cells and that the lack of iPSC-derived RPE maturation is due to inefficient ciliogenesis in these cells.

To uncover the role of the primary cilium in iPSC-RPE, we designed a protocol to manipulate primary cilia specifically during the maturation stage of iPSC-RPE differentiation. We utilized three previously published ciliogenesis modulators: aphidicolin, a tetracyclic antibiotic that increases ciliogenesis by blocking the G1-to-S transition in cells (Lancaster et al., 2011); prostaglandin E2 (PGE2), an eicosanoid that enhances ciliogenesis by increasing intraflagellar transport (Jin et al., 2014); and HPI-4, an AAA+ ATPase dynein motor inhibitor that works in an opposite manner to PGE2 by blocking ciliary protein

transport to inhibit function of the cilium, providing a good negative control (Firestone et al., 2012). Fully confluent iPSC-RPE was treated for 4 weeks in serum-containing medium during the maturation phase of differentiation with either aphidicolin or PGE2 to enhance ciliogenesis or HPI-4 to suppress the primary cilium function. In comparison with untreated or HPI-4-treated cells, aphidicolin and PGE2 enhanced ciliogenesis (ARL13B and GT335) and increased the number of cilia in a confluent RPE monolayer (Figures 1E–1H). Although HPI-4 treatment did not decrease the number of cilia, it suppressed cilium function by inhibiting intraflagellar protein transport. This was confirmed by reduced expression of two known ciliary axoneme proteins, IFT88 and GLI2, in HPI-4-treated cells (Figures S1A–S1H; Hay-craft et al., 2005; Pazour et al., 2000). It is worth noting that RPE cells derived from three different iPSC lines (Table S1) produced comparable data across these treatments and other experiments presented throughout this manuscript.

As expected, enhanced ciliogenesis by either aphidicolin or PGE2 significantly improved structural maturation of cells with increased pigmentation and extensive apical processes, as confirmed by transmission electron microscopy (TEM) (Figures 1I–1L) and scanning electron microscopy (Figures S1I–S1L). A readout of epithelial maturity is a homogeneous and elevated expression of maturity and polarity markers across the entire epithelial monolayer. We examined the expression of EZRIN, a polarity marker, and RPE65, a maturity marker, by immunostaining. In both aphidicolin- and PGE2-treated cells, but not in untreated or HPI-4-treated cells, the expression of both of these proteins was dramatically increased and expressed homogeneously throughout all cells in the iPSC-RPE monolayer (Figures 1M–1P and Figures S1M–S1P). Consistent with improved structural and molecular maturation of individual cells, both aphidicolin and PGE2 treatment improved functional maturation of the RPE monolayer (Figures 1Q–1U). Transepithelial potential (TEP), a difference in membrane potential of apical and basal membranes, reflects the differential expression of ion channels on either membrane. A higher TEP reflects enhanced functional polarization and maturation of the RPE monolayer. Compared with the untreated RPE monolayer (TEP of 2.66 ± 0.27 mV) or HPI-4-treated monolayer (TEP of 0.14 ± 0.66 mV), both aphidicolin- and PGE2-treated cells had significantly increased TEP (4.31 ± 0.33 mV and 5.87 ± 0.26 mV, respectively) (Figures 1Q–1U; Table S2). Furthermore, treatment with aphidicolin or PGE2 improved the hyperpolarization responses of the RPE monolayer in response to reduced apical potassium concentration from 5 mM to 1 mM, a physiological stimulus that mimics the subretinal space K^+ concentration drop upon dark-to-light transition and induces RPE apical membrane hyperpolarization (Joseph and Miller, 1991) compared with untreated controls or HPI-4-treated cells. Aphidicolin- and PGE2-induced changes in RPE monolayer TEP were similar in response to native human RPE (Adijanto et al., 2009) and consistent with increased expression of the RPE potassium channel KCNV2, as seen on the broader gene expression panel (Figure 1X). To further determine the functional maturity of cells, we tested the ability of RPE cells to phagocytose photoreceptor outer segments, one of the most critical functions of RPE cells (Bharti et al., 2011). Treatment of aphidicolin made RPE cells 2–3 times more phagocytic compared with untreated cells, confirming the notion that ciliogenesis improves the functional maturity of iPSC-RPE cells (Figure 1V).

To further understand the effect of the primary cilium induction on RPE maturation and determine whether cilium modulation shifted iPSC-RPE gene expression to more adult-like cells, we performed a comprehensive gene expression analysis of 71 previously identified fetal RPE-specific and 88 adult RPE-specific genes (Strunnikova et al., 2010). Compared with untreated cells, treatment with aphidicolin and PGE2 shifted the global pattern of RPE-specific gene expression toward less fetus-specific (aphidicolin, 72%; PGE2, 63%) and more adult-specific (aphidicolin, 51%; PGE2, 53%) genes. In contrast, HPI-4 treatment led to a significant downregulation of all RPE genes (Figures 1W and 1X; Table S3). This suggests that structural and functional changes seen in RPE monolayers treated with cilium-modulating drugs is likely due to changes in levels of RPE-specific genes. Overall, these data confirmed that experimentally enhanced ciliogenesis generates fully mature and polarized iPSC-RPE cells, whereas functional inhibition of cilia does not allow iPSC-RPE to mature.

Primary Cilium-Induced iPSC-RPE Maturation Is Mediated by Canonical WNT Suppression and Recruitment of Key Canonical WNT Effectors to the Base of the Cilium

RPE fate commitment requires temporally regulated canonical WNT signaling; WNT over-activation in mouse RPE leads to patterning defects (Fujimura et al., 2009; Westenskow et al., 2009). The primary cilium suppresses canonical WNT signaling by inducing the degradation of cytoplasmic β -catenin, resulting in depletion of the transcriptionally active nuclear form, and translocation of inactive β -catenin to tight junctions (Lancaster et al., 2011; MacDonald et al., 2009). Based on this literature evidence, we asked whether primary cilium-induced iPSC-RPE maturation is caused by canonical WNT suppression. In contrast to untreated or HPI-4-treated hiPSC-RPE, both aphidicolin and PGE2 treatment increased translocation of cytoplasmic β -catenin to the membrane, suggesting canonical WNT suppression (Figures 2A–2D). Consistently, both aphidicolin and PGE2-treated cells showed reduced rates of proliferation, as confirmed by Ki67 immunostaining (Figures 2E–2H), and significantly enhanced cell cycle exit, as seen by increased p27^{kip1} expression (Figures 2I–2L). For post-mitotic cells such as RPE cells, cell cycle exit is required for complete maturation. Therefore, these results suggest that, downstream of primary cilia, canonical WNT suppression-mediated cell cycle exit is one key pathway to induce RPE maturation.

To gain further mechanistic insights into the role of primary cilia in suppressing the canonical WNT pathway, we looked at the expression and localization of the canonical WNT modulators INVERSIN and JOUBERIN, which have previously been shown to be associated with primary cilia (Lancaster et al., 2011; Simons et al., 2005). We determined that suppression of β -catenin transcriptional activity in aphidicolin- or PGE2-treated samples was likely due to enhanced recruitment of the β -catenin inhibitor INVERSIN and co-activator JOUBERIN to the cilium compared with HPI-4-treated cells, where the two proteins predominantly localized to the membrane or the cytoplasm (Figures 2M–2T). Enhanced recruitment of INVERSIN to the ciliary base is likely due to its direct physical interactions with the ciliary trafficking protein BBS8 (Figure 2U). In co-immunoprecipitation assays, INVERSIN was able to co-immunoprecipitate with BBS8. Direct involvement of the primary cilium and its components in suppression of canonical WNT signaling is further confirmed in BBS8 knockdown RPE cells, in which increased

phosphorylation of transcriptionally active serine 552 on β -catenin is observed (Figure S2A). Consistent with the above data, aphidicolin and PGE2 treatments suppressed more than 80% of canonical WNT target genes, and HPI-4 lead to their increased activation (Figure 2V; Figure S2B). These results strongly support the hypothesis that the complete RPE maturation seen with enhanced ciliogenesis in hiPSC-RPE results from a direct suppression of canonical WNT signaling by ciliary proteins, forcing cell cycle exit to induce RPE maturation.

It is worth noting that our observations in iPSC-RPE are likely not due to cilia affecting SHH signaling (Sasai and Briscoe, 2012). HPI-4 inhibition of RPE maturation is independent of its effect on SHH suppression because a known SHH inhibitor, cyclopamine (Taipale et al., 2000; Tuson et al., 2011), did not affect RPE maturation in this assay (data not shown).

Canonical WNT Suppression Alone Is Not Sufficient to Induce iPSC-RPE Maturation

To determine whether canonical WNT suppression alone in the absence of primary cilium enhancers was sufficient to induce RPE maturation, we tested several known WNT inhibitors for their ability to suppress the canonical WNT pathway in iPSC-RPE. From this screen (data not shown), we identified two drugs that, when used together, led to a strong translocation of β -catenin from the nucleus to the cell membrane, suppressing canonical WNT activity. IWP2 renders WNT ligands inactive by blocking their palmitoylation through suppression of the acyltransferase enzyme PORCUPINE and also inhibits canonical WNT co-receptor LRP6, thus blocking β -catenin nuclear accumulation (Yeh and Peterson, 2009). Endo-IWR1 stabilizes the β -catenin destruction complex by interacting with AXIN, thus blocking β -catenin accumulation (Chen et al., 2009). For comparison, we used a well-known canonical WNT activator, CHIR99201, which works opposite to endo-IWR1, inhibits GSK3, and leads to β -catenin stabilization (Leach et al., 2015). As expected and as compared with untreated cells, treatment with IWP2+endo-IWR1 led to stronger translocation of β -catenin to the plasma membrane, whereas CHIR99201 treatment enhanced β -catenin localization in the nucleus (Figures 3A–3C). Treatment with IWP2+endo-IWR1 led all cells in the monolayer to exit the cell cycle with high nuclear p27^{kip1} expression compared with untreated or CHIR99201-treated cells (Figures 3D–3F). Consistent with enhanced cell cycle exit, IWP2+endo-IWR1-treated cells expressed higher levels of the maturation marker RPE65 (Figures 3G–3I). Furthermore, TEM analysis confirmed the presence of extensive apical processes on cells where canonical WNT signaling was turned off compared with untreated or CHIR99201-treated cells (Figures 3J–3L). These structural and molecular changes in iPSC-RPE cells were also evident in a functional analysis of IWP2+endo-IWR1-treated cells displaying four times higher phagocytosis activity compared with untreated or CHIR99201-treated cells (Figure 3M). Although canonical WNT suppression in the absence of cilium enhancers led to cell cycle exit, increased expression of mature RPE genes, and increased rate of phagocytosis in iPSC-RPE, it did not lead to complete maturation and polarization of the RPE monolayer. For instance, the hyperpolarization response and changes in RPE TEP caused by a 5 mM to 1 mM potassium concentration drop was not evident in IWP2+endo-IWR1-treated cells (Figure 3N; Table S2). Taken together, our results demonstrate that,

although canonical WNT suppression is necessary for RPE maturation, it is not sufficient for this effect.

Primary Cilium-Induced iPSC-RPE Functional Polarization Is Mediated through PKC δ Activation

The inability of canonical WNT suppression alone to induce complete RPE polarization prompted us to investigate other pathways that might be influencing RPE maturation downstream of the primary cilium. Apical-basal polarization of epithelial cells is triggered by actin-cytoskeleton alignment along the circumferential axis of the cell, isolating apical and basolateral membrane domains and their respective channel proteins. This process is regulated by a protein kinase, PKC δ (Kinoshita et al., 2003; Kühl et al., 2000). We therefore investigated the role of PKC δ in RPE maturation. In iPSC-RPE, aphidicolin enhanced ciliogenesis activated PKC δ , translocating it to the cell membrane and to the base of the primary cilium (Figures 4A–4C), likely through direct protein-protein interactions with the ciliary trafficking protein BBS8, as confirmed by co-immunoprecipitation between BBS8 and PKC δ (Figure 4D; Figure S3A). Phospho-Myosin Light Chain 2 (pMLC2), a downstream effector of PKC δ (Jamison et al., 2013), was increasingly organized along cell boundaries in aphidicolin-treated cells (Figures 4E and 4F), suggesting an increased activity of PKC δ in cells with enhanced ciliogenesis. Rottlerin, a specific PKC δ inhibitor, completely blocked aphidicolin-induced organization of pMLC2 along cell boundaries (Figure 4G), suggesting a prominent role of this kinase in inducing RPE polarization downstream of primary cilia. Consistent with the blockage of PKC δ activity, rottlerin treatment suppressed aphidicolin-induced enhancement of RPE apical processes (Figures 4H–4J). The most striking phenotype of PKC δ inhibition is seen in iPSC-RPE functional polarization responses and the ability of cells to hyperpolarize in response to reduced potassium concentration and to depolarize in response to ATP. Rottlerin treatment of control cells and cells previously treated with aphidicolin dampened RPE monolayer electrical responses in a dose-dependent manner (Figures 4K–4R; Figure S3B). Similar data were obtained using another PKC δ inhibitor, GÖ6850 (Table S2). These results suggest that, in addition to canonical WNT suppression, primary cilium-induced apical process maturation and functional polarization in RPE cells are mediated by PKC δ activation.

Primary Cilium Induction Helps Generate Mature and Polarized Lung Epithelial Cells

Primary cilia are present on several other epithelial cells types (Jain et al., 2010; May-Simera et al., 2015; Mirzadeh et al., 2010; Mitchell et al., 2009). The effects of enhanced ciliogenesis on iPSC-RPE maturation prompted us to investigate a similar role for primary cilia on other specialized epithelia derived from different germ layers. We differentiated iPSCs into proximal lung epithelial cells (iPSC-PLECs) using modification of a previously published protocol (Firth et al., 2014). iPSCs were first differentiated into definitive endoderm (FOXA2), followed by anterior endoderm (NKX2.1), and finally into iPSC-PLECs (CC10/FOXJ1) (Figures S4A–S4D). Similar to iPSC-RPE, treating precursor iPSC-PLECs with aphidicolin enhanced ciliogenesis, as confirmed by ARL13B immunostaining (Figures 5A and 5B; GT335 and acetylated tubulin not shown). Furthermore, treatment with aphidicolin improved tight junctions, as seen by increased ZO-1 immunostaining (Figures 5C and 5D) and enhanced apical process formation, as confirmed by EZRIN

immunostaining (Figures 5E and 5F). Similar to iPSC-RPE, cilium-induced iPSC-PLEC maturation is likely also mediated by canonical WNT suppression, as confirmed by reduced nuclear localization of β -catenin in aphidicolin-treated iPSC-PLECs compared with untreated cells (Figures 5G and 5H). Overall, our results confirm a broader role for the primary cilium in polarization of iPSC-derived epithelial cells and suggests that pharmacological enhancement of ciliogenesis may be a strategy to improve the differentiation of other iPSC-derived tissues.

Knockdown of the Cilium Protein IFT88 Severely Compromises iPSC-RPE Monolayer Maturity

To genetically confirm our findings obtained with pharmacological manipulation of cilia and to further understand the mechanistic basis of primary cilium-mediated RPE maturation, we targeted a ciliary trafficking gene, IFT88 (Pazour et al., 2000). Lentivirus-based short hairpin RNA (shRNA) reduced IFT88 expression to approximately 40% of wild-type levels in mono-layers of wild-type iPSC-RPE (Figure 6A). Consistent with the level of knockdown, ARL13B immunostaining confirmed that ciliogenesis was compromised in IFT88-KD-iPSC-RPE mono-layer (Figures 6B and 6C). Similar to HPI-4- or rottlerin-treated cells, IFT88 knockdown RPE showed severe maturation and functional polarization defects. Broad gene expression analysis demonstrated reduced expression of a majority of RPE signature genes (58% of 160 genes) and adult RPE-specific genes (45% of 70 genes; Figure 6D). ZO-1 immunostaining revealed that IFT88 knockdown iPSC-RPE had severe tight junction defects and reduced expression of cyclin-dependent kinase inhibitor 1B (p27^{kip1}) (Figures 6E and 6F), suggesting that, unlike ciliogenesis-enhanced cells, IFT88 knockdown cells are not able to fully exit the cell cycle or form mature junctional complexes. Scanning electron microscopy confirmed that, just like HPI-4- or rottlerin-treated cells, IFT88 knockdown iPSC-RPE has acutely underdeveloped apical processes (Figures 6G and 6H) with significantly reduced expression of the apical process and polarization marker EZRIN (Figures 6I and 6J). To confirm whether these structural polarization defects also affect iPSC-RPE functional polarization, we measured TEP. Compared with scrambled shRNA controls (TEP 0.96 ± 0.05 mV), IFT88-KD-iPSC-RPE displayed close to zero TEP (0.06 ± 0.05 mV), suggesting complete loss of functional apical-basal polarity (Figures 6K and 6L; Table S4). Furthermore, compared with control cells, IFT88-KD-iPSC-RPE barely responded to apical extracellular low K^+ (IFT88 knockdown [KD], 0.14 ± 0.03 mV; control, 0.92 ± 0.06 mV; $n = 5$) and the stimulation of apical P2Y2 receptors by ATP (IFT88 KD, 0.10 ± 0.04 mV; control, 0.74 ± 0.09 mV; $n = 5$) that activates intracellular signals needed for RPE membrane polarization (Peterson et al., 1997; Figures 6K and 6L; Table S4). Treatment of IFT88 KD cells with aphidicolin only partially rescued the TEP responses of RPE cells, likely because of slightly improved ciliogenesis in cells where IFT88 knockdown was not very effective (note the incomplete IFT88 KD across the RPE monolayer in Figures 6A–6C). These results suggest that, similar to the defects observed in HPI-4- or rottlerin-treated cells, reducing IFT88 expression in wild-type (WT) iPSC-RPE severely compromises their maturity and functional apical-basal polarity, further underscoring a role for primary cilia in this process and providing support for data obtained using pharmacological modulators of cilia.

RPE Cells Derived from Ciliopathy Patients with Joubert Syndrome Show Defective Structural and Functional Maturity

Ciliopathy patients have severe retinal and photoreceptor degeneration (Bujakowska et al., 2017; Wheway et al., 2014), but it is not known whether the RPE of these patients has any developmental or functional abnormalities. To address this question, we generated iPSCs from a ciliopathy patient (Joubert syndrome) with mutations in the ciliary gene CEP290. CEP290 encodes a key cilium transition zone protein involved in the regulation of ciliary protein composition (Coppieters et al., 2010; Craige et al., 2010; Rachel et al., 2012). CEP290-iPSCs were generated from a 3-year-old patient with biallelic nonsense mutations in CEP290 (17-bp deletion c.2495_2512 del/InATCT and c.5668 G > T substitution; Figures 6M and 6N; Table S1). The patient presented with delayed development, a classic “molar tooth sign” in the midbrain, 20/800 binocular acuity, oculomotor apraxia, horizontal nystagmus, midperipheral coloboma in the left retina/choroid, and pigmentary changes suggesting retinal degeneration. Renal function was normal to date with loss of corticomedullary differentiation. CEP290-iPSCs differentiated into RPE with an efficiency comparable with control iPSCs (data not shown) (Miyagishima et al., 2016). Although fully confluent CEP290-iPSC-RPE formed primary cilia similar to the control, CEP290 expression in patient iPSC-RPE was reduced compared with control iPSC-RPE with no detectable CEP290 protein at the ciliary base (Figures 6O–6Q). It is surprising that, despite premature stop codon mutations in both alleles, approximately 10% CEP290 expression was still detected (see Discussion for details; this 10% expression is likely due to mutant exon skipping that has been observed previously with CEP290 mutants) (Drivas et al., 2015). The number of cilia was similar (data not shown), but the cilium size was consistently smaller in patient cells compared with control cells, as confirmed by the cilia markers ARL13B and GT335 (healthy, $1.57 \pm 0.66 \mu\text{m}^2$; patient, $0.92 \pm 0.47 \mu\text{m}^2$) (Figures 6R–6T). RPE monolayer analysis revealed that, similar to IFT88 KD and HPI-4-treated iPSC-RPE, patient cells had irregular ZO-1 staining compared with healthy sibling cells (Figures S5A and S5B). This suggests that tight junction assembly defects in patient iPSC-RPE likely also resulted from incomplete maturation because of defective cilia. As expected, incompletely matured patient RPE phagocytosed three times fewer photoreceptor outer segments (Figure 6U). These maturation and functional defects prompted us to investigate RPE apical processes. Again, similar to IFT88 KD iPSC-RPE and HPI-4-treated iPSC-RPE, scanning electron microscopy confirmed abnormal (blebbed instead of typical finger-like) apical processes (Figures 6V and 6W; Miyagishima et al., 2016) Furthermore, quantitative gene expression analysis of patient cells confirmed incomplete maturation of CEP290-iPSC-RPE and revealed downregulation of RPE signature genes (74% of 160 genes; specific examples include the gap junction protein CX43, the visual cycle enzyme RDH11, the chloride channel CLCN4, and the pigmentation gene TYRP1) and adult RPE-specific genes (67% of 70 genes; specific examples include the glucose transporter GLUT1, the visual cycle enzymes LRAT and ALDH1A3, and the extracellular matrix [ECM] components FBLN1 and TIMP3) in patient compared with healthy cells (Figures 6X and 6Y; Table S3; Strunnikova et al., 2010). However, unlike IFT88 KD, immunostaining did not show prominent differences in RPE65 and still retained patchy EZRIN expression in patient cells compared with healthy iPSC-RPE (Figures S5C and S5D; Table S3; data not shown). These data suggest that, although CEP290-iPSC-RPE initiate normal differentiation, they do not

attain complete maturity. Analysis of ciliopathy patient RPE confirmed our data obtained using cilium-modulating drugs and IFT88 KD iPSC-RPE, showing that the primary cilium is indeed critical for the maturation and functional polarization of RPE cells. It also demonstrated that, in addition to photoreceptor degeneration, ciliopathy patients have RPE maturation defects that might contribute to the retinal degeneration phenotype.

RPE Maturation Defects in a Ciliopathy Mouse Model Precede Photoreceptor Degeneration

Although the analysis of ciliopathy patient iPSC-RPE confirmed maturation defects in these cells, it did not provide information about the temporal sequence of events. We asked which of the two cell types, RPE or photoreceptors, first shows changes in maturation and functional properties. To address this question, we used a mouse ciliopathy model. Photoreceptor outer segment development in mice begins around post-natal day 5 (P5), with complete maturation by P21. In contrast, RPE maturation is completed by P0 (Bharti et al., 2012; Nasonkin et al., 2013). This temporal difference in RPE and photoreceptor maturation provided us with the possibility to investigate whether RPE defects precede the photoreceptor degeneration seen in mouse models with defective primary cilium.

We chose to work with the *TTC8* gene, which encodes for BBS8, a key component of the “Bbsome” required for protein trafficking into and out of the primary cilium (Nachury et al., 2007). *Bbs8* knockout mice with dysfunctional primary cilia recapitulate the human ciliopathy phenotype, including early-onset retinal degeneration (Tadenev et al., 2011). Furthermore, BBS8 is likely directly involved in primary cilium-mediated RPE maturation, and it interacts with the WNT inhibitor INVERSIN and with the apical-basal polarity-inducing kinase PKC δ (Figures 2Q and 4D). Therefore, we investigated whether *Bbs8*^{-/-} mice also present with RPE maturation defects, as seen in Joubert syndrome patient iPSC-RPE and IFT88 KD iPSC-RPE. We analyzed RPE maturation in *Bbs8*^{-/-} mice at P0, prior to photoreceptor differentiation or degeneration. In contrast to WT littermates, but similar to IFT88-KD-iPSC-RPE and CEP290-iPSC-RPE, the RPE in *Bbs8*^{-/-} mice displayed multiple signs of incomplete maturation. This included underdeveloped tight junctions, as confirmed by ZO-1 immunostaining and irregular localization of the cilium marker ROOTLETIN (Figures 7A and 7B). Scanning electron microscopy revealed apical process defects with sparse and underdeveloped processes (Figures 7C and 7D; Figures S6A–S6D). Analysis of apical processes in this mouse model revealed another critical feature of primary cilium regulation of RPE maturation. Apical process defects were more prominent in peripheral RPE compared with central RPE, suggesting a possible gradient of primary cilium activity across different RPE areas, a cellular phenotype that is missed in cultured cells. Lower expression of the maturation genes *Rpe65* and *Mertk* and higher expression of the developmental genes *Mitf*, *Pax6*, *Tyrp1*, *Tyrosinase*, and *E-Cadherin* further confirmed the notion of incomplete maturation in *Bbs8*^{-/-} RPE (Figures 7E–7G; Nasonkin et al., 2013). Consistent with abnormal RPE maturation, we observed a variable inter-nuclear distance between adjacent cells at P16, suggesting non-homogeneous monolayer development, likely because of variability in cell cycle exit (Figure S6E). Furthermore, at P16, we also observed significantly reduced melanosome transport into apical processes, a sign of defective maturation and polarization (Figure 7H). These results further confirmed the hypothesis that,

in vivo, primary cilium dysfunction leads to RPE maturation defects that precede the development or degeneration of photoreceptors of ciliopathy patients.

The *in vitro* results using cilium inducers and BBS8 KD in human RPE cells suggested that regulation of RPE maturation by the primary cilium via BBS8 is at least in part regulated by canonical WNT suppression. Therefore, we asked whether a similar pathway regulation exists in mouse RPE. Consistent with the data obtained from human cells, in *Bbs8*^{-/-} mouse RPE with defective cilia, β -catenin expression and nuclear localization were significantly increased, resulting in higher expression of several canonical WNT target genes in *Bbs8*^{-/-} RPE/choroid compared with the WT (Figures 7I and 7J; Figure S6F). These developmental defects and canonical WNT over-activation in *Bbs8*^{-/-} RPE further support the notion of a critical role for the primary cilium in suppressing canonical WNT activity in mouse RPE prior to its complete maturation.

DISCUSSION

Retinal degeneration is the most common phenotype among ciliopathy patients. Over 90 gene mutations have been linked to various kinds of ciliopathies, and retinal degeneration is associated with almost all of them (Braun and Hildebrandt, 2017; Bujakowska et al., 2017; Wheway et al., 2014). Most research on the retinal phenotype has focused on retinal photoreceptors that contain a highly specialized primary cilium that is found to degenerate in ciliopathy animal models and patients (Bujakowska et al., 2017; May-Simera et al., 2017). The contribution of other ciliated retinal cell types to retinal degeneration has not been investigated so far. The RPE is a ciliated monolayer epithelium that lies at the back of the eye and is essential for photoreceptor development and function. Here we provide genetic evidence using Jou-bert syndrome iPSC-RPE, IFT88 KD and *Bbs8*^{-/-} mouse, and pharmacology evidence that ciliogenesis enhances RPE maturation and functional polarization. Together, patient and mouse model data provide strong evidence that, in ciliopathy patients, RPE maturation defects precede photoreceptor degeneration. Furthermore, we demonstrate that, mechanistically, RPE maturation is mediated by canonical WNT suppression and PKC δ activation, which lead to actin-cytoskeletal rearrangements underlying apical-basal polarization. Finally, we show that pharmacological enhancement of ciliogenesis can be used to improve the differentiation of iPSC-derived epithelial cells and demonstrate fully mature adult-like structural and functional features. Such fully mature cells provide effective disease models, drug screening tools, and a potential cell therapy for AMD.

Defects in RPE maturation severely compromise RPE function, as confirmed by defective phagocytosis and the ability of RPE cells to respond to changes in extracellular potassium concentration (Figures 1Q–1T, 3M, 4K–4R; 6K and 6L, and 6U). Considering that all RPE functions, including phagocytosis and low potassium response, are fundamentally critical for photoreceptor health and survival, one can conclude that the primary cilium defects in the RPE also contribute to the retinal degeneration observed in ciliopathy patients and animal models. RPE defects temporally precede photoreceptor defects in *Bbs8*^{-/-} mice, further underscoring the importance of the RPE in the retinal degeneration seen in ciliopathy patients. Ciliopathy patients receive a “double hit”; the first from incompletely mature RPE

and the second from defective function of the cilium in the photoreceptor. In support of this, RPE defects are already observed in *Bbs8* knockout mice even before photoreceptors start maturing or begin to extend their connecting cilium and outer segments (Figures 7A–7F).

Multiple CEP290 mutations with distinct ciliopathy phenotypes have been identified (Coppieters et al., 2010). Although the precise function of CEP290 is still unknown, it is proposed to function at the ciliary transition zone and regulate ciliary trafficking (Rachel et al., 2012). The bi-allelic mutations identified in our patient with severe retinal degeneration are predicted to cause premature stop co-dons. However, patient iPSC-RPE continued to express ~10% of WT CEP290 protein (Figure 6O). This suggests that one or both exons with mutations are partially skipped during RNA splicing, a process reported for some other CEP290 mutations (Drivas et al., 2015). A 90% reduction in CEP290 protein levels contrasts our results with a recently published CEP290-iPSC manuscript, where the authors did not note any changes in RPE CEP290 expression and noticed defective photoreceptor maturation but no RPE maturation defects (Parfitt et al., 2016). This suggests a differential sensitivity of RPE and photoreceptors to CEP290 mutations and prompts the analysis of RPE phenotype in other ciliopathy patients and animal models. In the future, we plan to use isogenic iPSC lines with specific mutations to address whether the variability associated with CEP290 mutations and the age of retinal degeneration onset is due to certain mutations affecting both RPE and photoreceptors and others only affecting the photoreceptors (Coppieters et al., 2010).

Regulation of WNT signaling by primary cilia has not been easy to define, possibly because of spatial and temporal differences between tissues and cell types (May-Simera et al., 2015). Here we demonstrate that the primary cilium suppresses canonical WNT signaling during RPE maturation. We provide mechanistic insights into this pathway and show that WNT suppression is required for RPE maturation, although WNT suppression alone is not sufficient for RPE maturation (Figure 3). We provide additional mechanistic evidence that WNT signaling suppression is directly regulated by the primary cilium (Figure 2). The cilium protein BBS8 directly recruits the canonical WNT repressor INVERSIN to the ciliary base, leading to DISHEVELLED degradation, β -catenin destruction complex activation, and β -catenin degradation, causing cell cycle exit (Lienkamp et al., 2012). Gene expression data from mouse RPE with defective cilia and hiPSC-RPE with pharmacologically defective cilia showed a higher expression of canonical WNT target genes compared with the control. Conversely, enhancement of ciliogenesis during RPE maturation lead to suppression of WNT target genes.

Canonical WNT suppression in the absence of enhanced ciliogenesis showed that, although WNT suppression is required, alone it is not sufficient to cause RPE maturation. Maturation and polarization of epithelial cells are triggered by actin-cytoskeleton alignment along the circumferential axis of the cell, isolating apical and basolateral membrane domains and their respective channel proteins. This process is regulated by a protein kinase, PKC δ (Kinoshita et al., 2003; Kühl et al., 2000). We show here that, in RPE cells, PKC δ activation is regulated by the primary cilium. The BBS8-PKC δ interaction recruits PKC δ to the base of the primary cilium, likely leading to its activation. Activated PKC δ leads to Myosin Light Chain 2 phosphorylation and actin cytoskeleton alignment along cell boundaries. This, in

turn, reinforces tight junctions and isolates apical and basolateral membranes. Isolated apical and basolateral membranes result in distinct ion channel distribution on the two sides, leading to functional polarization. One of the best readouts of this process is the measurement of TEP, which reflects the differential expression of apical and basal ion channels and is an indicator of polarization across the epithelial monolayer. IFT88-KD-iPSC-RPE and HPI-4-treated cells with dysfunctional cilia lacked apical-basal polarity with no detectable TEP, whereas aphidicolin- and PGE2-treated cells with enhanced cilia had high TEP, similar to the native tissue (Quinn and Miller, 1992). Inadequate ciliogenesis, therefore, leads to incomplete polarization across the entire epithelial monolayer.

The function of PKC δ identified here is likely independent of its known role in the planar cell polarity (PCP) pathway but is regulated via a calcium-dependent pathway (Kühl et al., 2000). BAPTA (1,2-bis(o-aminophenoxy)ethane-N,N,N',N'-tetraacetic acid), a calcium chelator, reduced aphidicolin-induced electrical responses in iPSC-RPE (Table S2). Similarly, our observations in iPSC-RPE are likely not due to cilia affecting SHH signaling (Sasai and Briscoe, 2012). HPI-4 is known to affect both SHH and the cilium function (Firestone et al., 2012), but inhibition of RPE maturation by HPI-4 is independent of its effect on SHH suppression. A known SHH inhibitor, cyclopamine (Taipale et al., 2000; Tuson et al., 2011), did not change RPE maturation or functional polarization (data not shown). Furthermore, similar to aphidicolin, HPI-4 also blocks the cell cycle, but it does so by inhibiting dynein motors, not by promoting ciliogenesis (Okayama, 2012). This unnatural cell cycle block (confirmed by weak p27^{kip1} expression) (Figure 2L) fails to mature iPSC-RPE, suggesting that cell cycle block per se is not sufficient to trigger RPE maturation. Activation of ciliogenesis in the RPE causes a natural cell cycle exit that is required for complete cell maturation.

Apical processes, a hallmark feature of RPE polarization, are strongly affected by ciliogenesis. Furthermore, in the ciliopathy mouse model, we identified possible region-specific differences in primary cilium regulation of apical process development. *Bbs8*^{-/-} mouse RPE has defective apical processes predominantly in the periphery, less so in the center part of the eye. To our knowledge, this is the first identified pathway with differential effects on peripheral versus central RPE. Further analysis of this effect may provide more insight into the development of the human macula, the central area of the eye with highest visual acuity, and retinal degenerative diseases. It is currently not clear how ciliogenesis leads to synchronous apical process formation in the RPE. It is possible that it is linked to cytoskeleton re-alignment along cell boundaries and/or that cilia proteins directly regulate protein trafficking into apical processes. Consistent with the latter idea, a punctate distribution of CEP290 was noted throughout the apical cytoplasm in WT iPSC-RPE (Figure 6P). We are currently further investigating this observation.

Because we were able to improve the maturation and polarization of iPSC-RPE cells via modulation of the primary cilium, we tested whether a similar approach could also enhance maturation of other iPSC-derived epithelial tissues. Because a similar improvement was seen in the maturation of iPSC-derived proximal lung epithelial cells, it strengthened our hypothesis that the primary cilium provides a developmental role in at least more than one

epithelial cell polarization. We propose that the differentiation of many other tissues may benefit from the modulation of primary cilia.

In conclusion, we show that ciliogenesis is a mechanism with which to mature iPSC-derived RPE and lung epithelia. This work has helped develop mature and polarized iPSC-RPE for autologous cell therapy of AMD patients and also highlights other considerations when developing treatment strategies for retinal degeneration in ciliopathy patients—that a combined defect in RPE and photoreceptors likely underlies the mechanism for ciliopathy-induced retinal degeneration—and suggests a cautionary note for gene therapy trials that aim to only target photoreceptors because they may only work in select mutations that do not affect the RPE.

EXPERIMENTAL PROCEDURES

Mice

The generation and genotyping of *Bbs8*^{-/-} mutant mice have been described previously (Tadenev et al., 2011). For embryonic staging, the morning after mating was considered embryonic day (E) 0.5.

Generation, Characterization, and Differentiation of hiPSCs

Cells isolated from donor tissue were reprogrammed using Sendai virus-mediated delivery (CytoTune, Life Technologies) of the four Yamanaka factors (c-MYC, KLF4, OCT4, and SOX2), following the manufacturer's recommendations. Three-germ layer differentiation of iPSC lines was performed using a published protocol (Takahashi et al., 2009). Antibodies against NESTIN, TUJ1, SOX17, AFP, BRACHYURY, and SMA were used for characterization of cells of all three germ layers. Karyotyping was performed at Cell Line Genetics (Madison, WI). iPSCs were differentiated into RPE using a previously published protocol (Ferrer et al., 2014) with modifications (see the Supplemental Experimental Procedures). All human work was done under institutional review board-approved protocol #11-E1-0245.

Electrophysiological Recordings

Human primary RPE or iPSC-RPE monolayers were mounted on a modified Üssing chamber, and electrophysiology recordings were done as described previously (Maminishkis et al., 2006; Peterson et al., 1997).

Phagocytosis Assay

Isolation, preparation of photoreceptor outer segments, and the phagocytosis assay were performed as described previously (Mao and Finnemann, 2013).

Statistical Analysis

Most data were repeated in RPE cells derived from three iPSC lines. Oneway ANOVA was used for dose-dependent inhibition of PKC δ pharmacological blockers. Two-way repeated measures ANOVA was used with a Bonferroni correction for multiple comparisons of image quantification. Kolmogorov-Smirnov (K-S) test was used to compare the distributions

between different treatment conditions of a large set of gene expression. All other data were analyzed using unpaired, two-tailed Student's t test. Data were represented as mean \pm SEM and considered significantly different at $p < 0.05$.

Supplementary Material

Refer to Web version on PubMed Central for supplementary material.

ACKNOWLEDGMENTS

This work was supported by NEI intramural funds, NIH CRM, and NIH Common Fund grants (to K.B. and S.M.), and an Alexander von Humboldt Foundation grant (to H.L.M.-S. and S.P.). The authors thank Heinz Arnheiter, Tiziana Cogliati, and Jeffery Rubin for helpful comments and Viola Kretschmer, Alur Prasad, and Sunit Dutta for technical assistance.

REFERENCES

- Adijanto J, Banzon T, Jalickee S, Wang NS, and Miller SS (2009). CO₂-induced ion and fluid transport in human retinal pigment epithelium. *J. Gen. Physiol* 133, 603–622. [PubMed: 19468075]
- Bharti K, Miller SS, and Arnheiter H (2011). The new paradigm: retinal pigment epithelium cells generated from embryonic or induced pluripotent stem cells. *Pigment Cell Melanoma Res.* 24, 21–34. [PubMed: 20846177]
- Bharti K, Gasper M, Ou J, Brucato M, Clore-Gronenborn K, Pickel J, and Arnheiter H (2012). A regulatory loop involving PAX6, MITF, and WNT signaling controls retinal pigment epithelium development. *PLoS Genet.* 8, e1002757. [PubMed: 22792072]
- Braun DA, and Hildebrandt F (2017). Ciliopathies. *Cold Spring Harb. Perspect. Biol* 9, a028191.
- Bujakowska KM, Liu Q, and Pierce EA (2017). Photoreceptor cilia and retinal ciliopathies. *Cold Spring Harb. Perspect. Biol* 9, 028274.
- Chen B, Dodge ME, Tang W, Lu J, Ma Z, Fan C-W, Wei S, Hao W, Kilgore J, Williams NS, et al. (2009). Small molecule-mediated disruption of Wnt-dependent signaling in tissue regeneration and cancer. *Nat. Chem. Biol* 5, 100–107. [PubMed: 19125156]
- Coppieters F, Lefever S, Leroy BP, and De Baere E (2010). CEP290, a gene with many faces: mutation overview and presentation of CEP290base. *Hum. Mutat* 31, 1097–1108. [PubMed: 20690115]
- Craig B, Tsao CC, Diener DR, Hou Y, Lechtreck KF, Rosenbaum JL, and Witman GB (2010). CEP290 tethers flagellar transition zone micro-tubules to the membrane and regulates flagellar protein content. *J. Cell Biol* 190, 927–940. [PubMed: 20819941]
- Denman-Johnson K, and Forge A (1999). Establishment of hair bundle polarity and orientation in the developing vestibular system of the mouse. *J. Neurocytol* 28, 821–835. [PubMed: 10900087]
- Dobell C (1932). *Antony van Leeuwenhoek and His "Little Animals"* (New York: Harcourt, Brace and Co).
- Drivas TG, Wojno AP, Tucker BA, Stone EM, and Bennett J (2015). Basal exon skipping and genetic pleiotropy: A predictive model of disease pathogenesis. *Sci. Transl. Med* 7, 291ra97.
- Ferrer M, Corneo B, Davis J, et al. (2014). A multiplex high-throughput gene expression assay to simultaneously detect disease and functional markers in induced pluripotent stem cell-derived retinal pigment epithelium. *Stem Cells Transl. Med* 3, 911–922. [PubMed: 24873859]
- Firestone AJ, Weinger JS, Maldonado M, Barlan K, Langston LD, O'Donnell M, Gelfand VI, Kapoor TM, and Chen JK (2012). Small-molecule inhibitors of the AAA+ ATPase motor cytoplasmic dynein. *Nature* 484, 125–129. [PubMed: 22425997]
- Firth AL, Dargitz CT, Qualls SJ, Menon T, Wright R, Singer O, Gage FH, Khanna A, and Verma IM (2014). Generation of multiciliated cells in functional airway epithelia from human induced pluripotent stem cells. *Proc. Natl. Acad. Sci. U.S.A* 111, E1723–E1730. [PubMed: 24706852]

- Fujimura N, Taketo MM, Mori M, Korinek V, and Kozmik Z (2009). Spatial and temporal regulation of Wnt/beta-catenin signaling is essential for development of the retinal pigment epithelium. *Dev. Biol* 334, 31–45. [PubMed: 19596317]
- Gerdes JM, Davis EE, and Katsanis N (2009). The vertebrate primary cilium in development, homeostasis, and disease. *Cell* 137, 32–45. [PubMed: 19345185]
- Grisanti L, Revenkova E, Gordon RE, and Iomini C (2016). Primary cilia maintain corneal epithelial homeostasis by regulation of the Notch signaling pathway. *Development* 143, 2160–2171. [PubMed: 27122169]
- Haycraft CJ, Banizs B, Aydin-Son Y, Zhang Q, Michaud EJ, and Yoder BK (2005). Gli2 and Gli3 localize to cilia and require the intraflagellar transport protein polaris for processing and function. *PLoS Genet.* 1, e53. [PubMed: 16254602]
- Jain R, Pan J, Driscoll JA, Wisner JW, Huang T, Gunsten SP, You Y, and Brody SL (2010). Temporal relationship between primary and motile ciliogenesis in airway epithelial cells. *Am. J. Respir. Cell Mol. Biol* 43, 731–739. [PubMed: 20118219]
- Jamison J, Lauffenburger D, Wang JC-H, and Wells A (2013). PKC δ localization at the membrane increases matrix traction force dependent on PLCg1/EGFR signaling. *PLoS ONE* 8, e77434. [PubMed: 24155954]
- Jin D, Ni TT, Sun J, Wan H, Amack JD, Yu G, Fleming J, Chiang C, Li W, Papierniak A, et al. (2014). Prostaglandin signalling regulates ciliogenesis by modulating intraflagellar transport. *Nat. Cell Biol* 16, 841–851. [PubMed: 25173977]
- Joseph DP, and Miller SS (1991). Apical and basal membrane ion transport mechanisms in bovine retinal pigment epithelium. *J. Physiol* 435, 439–463. [PubMed: 1722821]
- Kim S, and Dynlacht BD (2013). Assembling a primary cilium. *Curr. Opin. Cell Biol* 25, 506–511. [PubMed: 23747070]
- Kinoshita N, Iioka H, Miyakoshi A, and Ueno N (2003). PKC delta is essential for Dishevelled function in a noncanonical Wnt pathway that regulates Xenopus convergent extension movements. *Genes Dev.* 17, 1663–1676. [PubMed: 12842914]
- Kühl M, Sheldahl LC, Malbon CC, and Moon RT (2000). Ca²⁺/calmodulin-dependent protein kinase II is stimulated by Wnt and Frizzled homologs and promotes ventral cell fates in Xenopus. *J. Biol. Chem* 275, 12701–12711. [PubMed: 10777564]
- Lancaster MA, Schroth J, and Gleeson JG (2011). Subcellular spatial regulation of canonical Wnt signalling at the primary cilium. *Nat. Cell Biol* 13, 700–707. [PubMed: 21602792]
- Leach LL, Buchholz DE, Nadar VP, Lowenstein SE, and Clegg DO (2015). Canonical/ β -catenin Wnt pathway activation improves retinal pigmented epithelium derivation from human embryonic stem cells. *Invest. Ophthalmol. Vis. Sci* 56, 1002–1013.
- Lee JE, and Gleeson JG (2011). A systems-biology approach to understanding the ciliopathy disorders. *Genome Med.* 3, 59. [PubMed: 21943201]
- Lehmann GL, Benedicto I, Philp NJ, and Rodriguez-Boulan E (2014). Plasma membrane protein polarity and trafficking in RPE cells: past, present and future. *Exp. Eye Res* 126, 5–15. [PubMed: 25152359]
- Lienkamp S, Ganner A, and Walz G (2012). Inversin, Wnt signaling and primary cilia. *Differentiation* 83, S49–S55. [PubMed: 22206729]
- Luo N, West CC, Murga-Zamalloa CA, Sun L, Anderson RM, Wells CD, Weinreb RN, Travers JB, Khanna H, and Sun Y (2012). OCRL localizes to the primary cilium: a new role for cilia in Lowe syndrome. *Hum. Mol. Genet* 21, 3333–3344. [PubMed: 22543976]
- MacDonald BT, Tamai K, and He X (2009). Wnt/beta-catenin signaling: components, mechanisms, and diseases. *Dev. Cell* 17, 9–26. [PubMed: 19619488]
- Maminishkis A, Chen S, Jalickee S, et al. (2006). Confluent monolayers of cultured human fetal retinal pigment epithelium exhibit morphology and physiology of native tissue. *Invest. Ophthalmol. Vis. Sci* 47, 3612–3624. [PubMed: 16877436]
- Mao Y, and Finnemann SC (2013). Analysis of photoreceptor outer segment phagocytosis by RPE cells in culture. *Methods Mol. Biol* 935, 285–295. [PubMed: 23150376]
- May-Simera H, and Kelley MW (2012a). Examining planar cell polarity in the mammalian cochlea. *Methods Mol. Biol* 839, 157–171. [PubMed: 22218900]

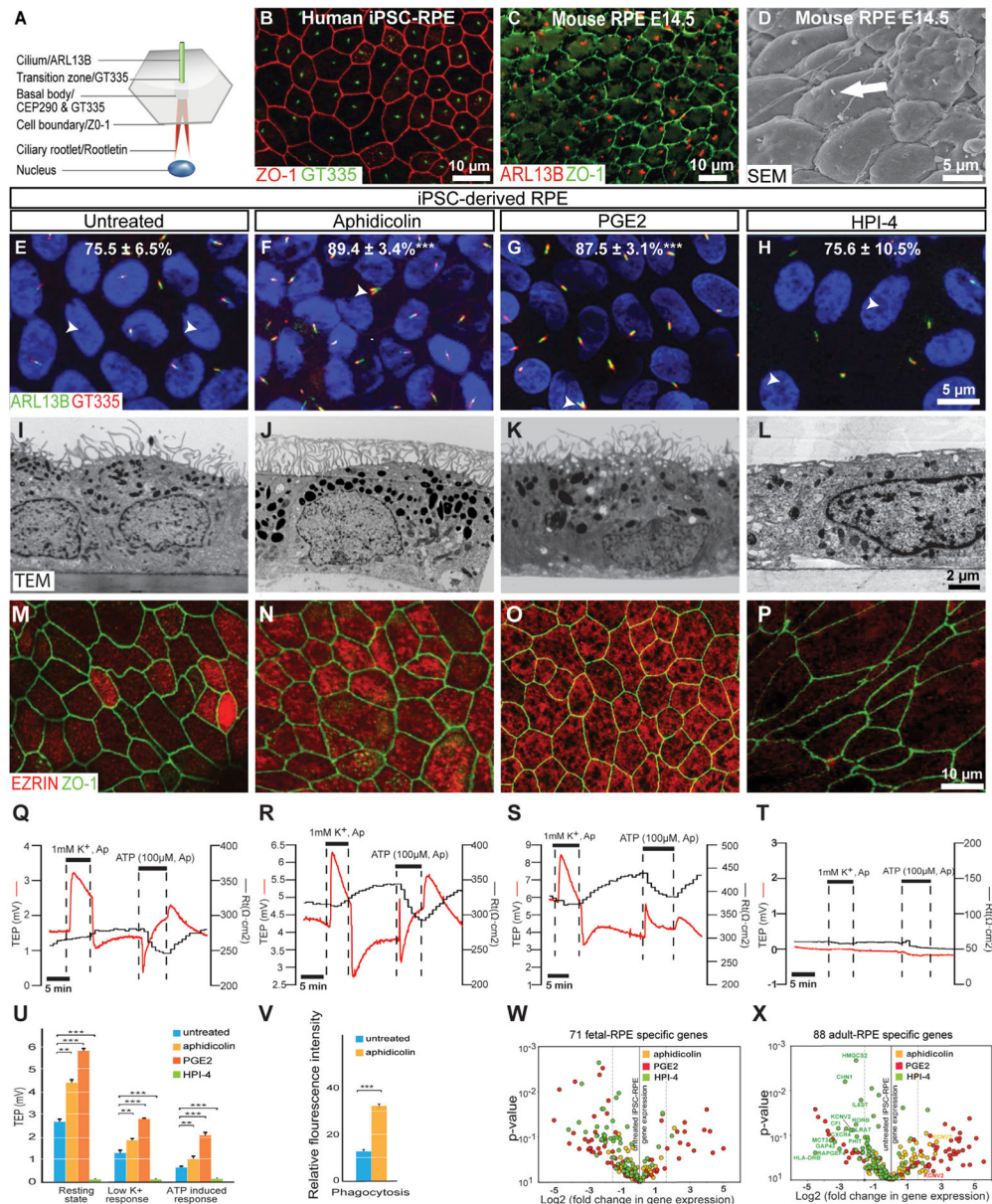
- May-Simera HL, and Kelley MW (2012b). Cilia, Wnt signaling, and the cyto-skeleton. *Cilia* 1, 7. [PubMed: 23351924]
- May-Simera HL, Petralia RS, Montcouquiol M, Wang Y-XX, Szarama KB, Liu Y, Lin W, Deans MR, Pazour GJ, and Kelley MW (2015). Ciliary proteins Bbs8 and Ift20 promote planar cell polarity in the cochlea. *Development* 142, 555–566. [PubMed: 25605782]
- May-Simera H, Nagel-Wolfrum K, and Wolfrum U (2017). Cilia - The sensory antennae in the eye. *Prog. Retin. Eye Res* 60, 144–180. [PubMed: 28504201]
- Mirzadeh Z, Han YG, Soriano-Navarro M, García-Verdugo JM, and Alvarez-Buylla A (2010). Cilia organize ependymal planar polarity. *J. Neurosci* 30, 2600–2610. [PubMed: 20164345]
- Mitchell B, Stubbs JL, Huisman F, Taborek P, Yu C, and Kintner C (2009). The PCP pathway instructs the planar orientation of ciliated cells in the *Xenopus* larval skin. *Curr. Biol* 19, 924–929. [PubMed: 19427216]
- Miyagishima KJ, Wan Q, Corneo B, Sharma R, Lotfi MR, Boles NC, Hua F, Maminishkis A, Zhang C, Blenkinsop T, et al. (2016). In pursuit of authenticity: Induced pluripotent stem cell-derived retinal pigment epithelium for clinical applications. *Stem Cells Transl. Med* 5, 1562–1574. [PubMed: 27400791]
- Muller OF (1786). *Animalcula infusoria; fluvia tilia et marina, que detexit, systematice descripsit et ad vivum delineari curavit Havniae: Typis N (Molleri).*
- Nachury MV, Loktev AV, Zhang Q, Westlake CJ, Peränen J, Merdes A, Slusarski DC, Scheller RH, Bazan JF, Sheffield VC, and Jackson PK (2007). A core complex of BBS proteins cooperates with the GTPase Rab8 to promote ciliary membrane biogenesis. *Cell* 129, 1201–1213. [PubMed: 17574030]
- Nasonkin IO, Merbs SL, Lazo K, Oliver VF, Brooks M, Patel K, Enke RA, Nelliserry J, Jamrich M, Le YZ, et al. (2013). Conditional knockdown of DNA methyltransferase 1 reveals a key role of retinal pigment epithelium integrity in photoreceptor outer segment morphogenesis. *Development* 140, 1330–1341. [PubMed: 23406904]
- Okayama H (2012). Cdc6: a trifunctional AAA+ ATPase that plays a central role in controlling the G(1)-S transition and cell survival. *J. Biochem* 152, 297–303. [PubMed: 22908236]
- Parfitt DA, Lane A, Ramsden CM, Carr A-JF, Munro PM, Jovanovic K, Schwarz N, Kanuga N, Muthiah MN, Hull S, et al. (2016). Identification and correction of mechanisms underlying inherited blindness in human iPSC-derived optic cups. *Cell Stem Cell* 18, 769–781. [PubMed: 27151457]
- Pazour GJ, Dickert BL, Vucica Y, Seeley ES, Rosenbaum JL, Witman GB, and Cole DG (2000). *Chlamydomonas* IFT88 and its mouse homo-logue, polycystic kidney disease gene *tg737*, are required for assembly of cilia and flagella. *J. Cell Biol* 151, 709–718. [PubMed: 11062270]
- Peterson WM, Meggyesy C, Yu K, and Miller SS (1997). Extracellular ATP activates calcium signaling, ion, and fluid transport in retinal pigment epithelium. *J. Neurosci* 17, 2324–2337. [PubMed: 9065493]
- Quinn RH, and Miller SS (1992). Ion transport mechanisms in native human retinal pigment epithelium. *Invest. Ophthalmol. Vis. Sci* 33, 3513–3527. [PubMed: 1334477]
- Rachel RA, Li T, and Swaroop A (2012). Photoreceptor sensory cilia and ciliopathies: focus on CEP290, RPGR and their interacting proteins. *Cilia* 1, 22. [PubMed: 23351659]
- Reiter JF, Blacque OE, and Leroux MR (2012). The base of the cilium: roles for transition fibres and the transition zone in ciliary formation, maintenance and compartmentalization. *EMBO Rep.* 13, 608–618. [PubMed: 22653444]
- Roignot J, Peng X, and Mostov K (2013). Polarity in mammalian epithelial morphogenesis. *Cold Spring Harb. Perspect. Biol* 5, a013789. [PubMed: 23378592]
- Ross AJ, May-Simera H, Eichers ER, Kai M, Hill J, Jagger DJ, Leitch CC, Chapple JP, Munro PM, Fisher S, et al. (2005). Disruption of Bardet-Biedl syndrome ciliary proteins perturbs planar cell polarity in vertebrates. *Nat. Genet* 37, 1135–1140. [PubMed: 16170314]
- Sasai N, and Briscoe J (2012). Primary cilia and graded Sonic Hedgehog signaling. *Wiley Interdiscip. Rev. Dev. Biol* 1, 753–772. [PubMed: 23799571]
- Simons M, Gloy J, Ganner A, Bullerkotte A, Bashkurov M, Krönig C, Schermer B, Benzing T, Cabello OA, Jenny A, et al. (2005). Inversin, the gene product mutated in nephronophthisis type II,

functions as a molecular switch between Wnt signaling pathways. *Nat. Genet* 37, 537–543. [PubMed: 15852005]

- Strunnikova NV, Maminishkis A, Barb JJ, Wang F, Zhi C, Sergeev Y, Chen W, Edwards AO, Stambolian D, Abecasis G, et al. (2010). Transcriptome analysis and molecular signature of human retinal pigment epithelium. *Hum. Mol. Genet* 19, 2468–2486. [PubMed: 20360305]
- Sugiyama Y, Stump RJ, Nguyen A, Wen L, Chen Y, Wang Y, Murdoch JN, Lovicu FJ, and McAvoy JW (2010). Secreted frizzled-related protein disrupts PCP in eye lens fiber cells that have polarised primary cilia. *Dev. Biol* 338, 193–201. [PubMed: 19968984]
- Tadenev ALD, Kulaga HM, May-Simera HL, Kelley MW, Katsanis N, and Reed RR (2011). Loss of Bardet-Biedl syndrome protein-8 (BBS8) perturbs olfactory function, protein localization, and axon targeting. *Proc. Natl. Acad. Sci. USA* 108, 10320–10325. [PubMed: 21646512]
- Taipale J, Chen JK, Cooper MK, Wang B, Mann RK, Milenkovic L, Scott MP, and Beachy PA (2000). Effects of oncogenic mutations in Smoothened and Patched can be reversed by cyclopamine. *Nature* 406, 1005–1009. [PubMed: 10984056]
- Takahashi K, Narita M, Yokura M, Ichisaka T, and Yamanaka S (2009). Human induced pluripotent stem cells on autologous feeders. *PLoS ONE* 4, e8067. [PubMed: 19956543]
- Tuson M, He M, and Anderson KV (2011). Protein kinase A acts at the basal body of the primary cilium to prevent Gli2 activation and ventralization of the mouse neural tube. *Development* 138, 4921–4930. [PubMed: 22007132]
- Westenskow P, Piccolo S, and Fuhrmann S (2009). Beta-catenin controls differentiation of the retinal pigment epithelium in the mouse optic cup by regulating Mitf and Otx2 expression. *Development* 136, 2505–2510. [PubMed: 19553286]
- Wheway G, Parry DA, and Johnson CA (2014). The role of primary cilia in the development and disease of the retina. *Organogenesis* 10, 69–85. [PubMed: 24162842]
- Yeh J-RJ, and Peterson RT (2009). Novel Wnt antagonists target porcupine and Axin. *Nat. Chem. Biol* 5, 74–75. [PubMed: 19148172]

Highlights

- Primary cilium-induced RPE maturation is mediated by WNT suppression and PKC δ activation
- iPSC-RPE cells derived from ciliopathy patients show defective structure and function
- RPE maturation defects in a ciliopathy mouse model precede photoreceptor degeneration
- Cilium-dependent maturation pathway also exists in iPSC-derived lung epithelium



respectively; arrowheads). Two-way repeated measures ANOVA with Bonferroni correction for multiple comparisons, 5 biological repeats for each group; *** $p < 0.001$.

(I–P) Treatment of iPSC-RPE with aphidicolin or PGE2 leads to enhanced apical processes (J and K) and increased EZRIN expression (red, N and O). In comparison, treatment with HPI-4 causes sparse apical processes (L) and low EZRIN expression (P), as compared to untreated samples (I and M).

(Q–U) Aphidicolin or PGE2 treatment largely increases the resting-state TEP of iPSC-RPE monolayers and dramatically enhances their electrical responses to physiological stimuli. In comparison, HPI-4 treatment seriously disrupts monolayer maturation. (Q–T) Representative traces. (U) Group data; $n = 22$ for control and $n = 19, 8,$ and 6 for aphidicolin-, PGE2-, and HPI-4-treated samples, respectively; ** $p < 0.01$, *** $p < 0.001$.

(V) Compared with untreated cells, aphidicolin treatment doubles the ability of iPSC-RPE to phagocytose photoreceptor outer segments (POs). *** $p < 0.001$, $n = 3$.

(W and X) Volcano plots of fetal (W) and adult (X) RPE-specific genes, showing that aphidicolin or PGE2 treatment decreases fetal-specific gene expression and increases adult-specific gene expression compared with untreated or HPI-4 treated cells. Genes most affected by HPI-4 treatment are highlighted.

3, 2, and 3 biological repeats for aphidicolin-, PGE2-, and HPI-4-treated samples, respectively.

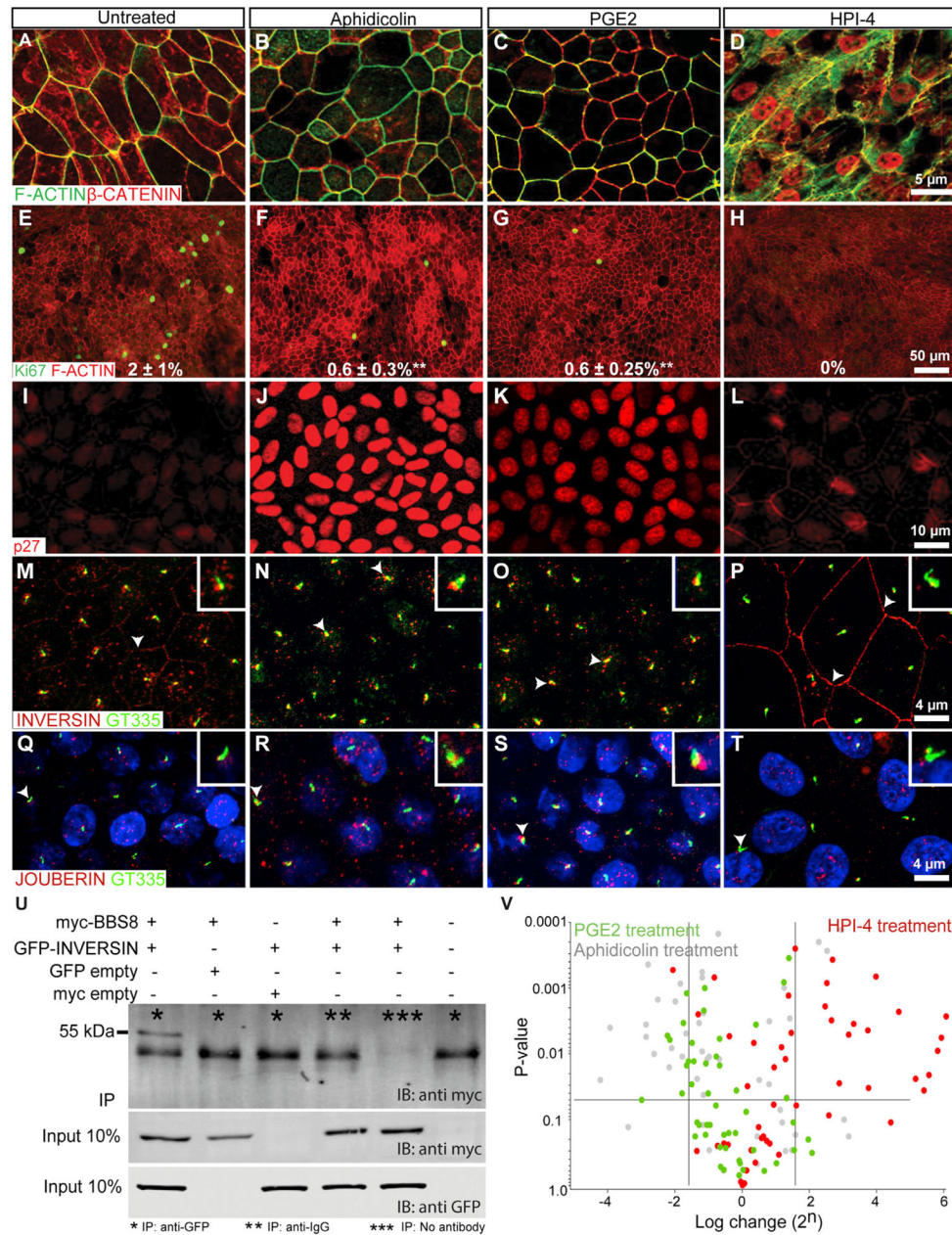


Figure 2. Experimentally Enhanced Ciliogenesis Promotes iPSC-RPE Monolayer Maturation through Canonical WNT Suppression and Cell Cycle Exit

(A–D) Aphidicolin (B) or PGE2 (C) treatment reduces cytoplasmic β-catenin (red) and improves epithelial morphology (F-actin, green) of iPSC-RPE compared with untreated (A) or HPI-4-treated (D) cells.

(E–H) Aphidicolin (F) or PGE2 (G) treatment decreases the number of dividing cells (Ki67, green) (two-way repeated measures ANOVA with Bonferroni correction for multiple comparisons, 5 biological repeats for all treatments; 2% ± 1% for untreated control (E), 0.6% ± 0.3% for aphidicolin-treated samples, **p < 0.01; 0.6% ± 0.25% for PGE2-treated

samples, $**p < 0.01$). Dividing cells are not observed after HPI-4 (H) treatment because it blocks the dynein motor needed for cell proliferation.

(I–L) Treatment of iPSC-RPE with aphidicolin or PGE2 (J and K) leads to high p27^{kip1} expression (red) relative to the untreated control (I). In comparison, treatment of HPI-4 causes low p27^{kip1} expression (L).

(M–P) Localization of the β -catenin inhibitor INVERSIN (red) to the cilium base (GT335, green) is stronger upon aphidicolin (N) and PGE2 (O) treatments (arrowheads) compared to untreated sample (M) and HPI-4 (P) treatment, where INVERSIN is mostly on the membrane (arrowheads).

(Q–T) Aphidicolin (R) and PGE2 (S) treatments recruit β -catenin co-activator JOUBERIN (red) to the cilium (GT335, green, arrowheads) stronger as compared to untreated (Q) and HPI-4 (T) treated samples.

(U) Physical interactions between BBS8-MYC and INVERSIN-GFP are confirmed by their co-immunoprecipitation from HEK293 cells co-expressing the two proteins. Negative controls: GFP- and MYC-expressing plasmids and rabbit immunoglobulin G (IgG).

(V) A volcano plot showing downregulation of canonical WNT genes in aphidicolin- and PGE2-treated iPSC-RPE compared with untreated cells. In contrast, HPI-4 treatment increases the expression of canonical WNT genes.

3 biological repeats for all samples were used.

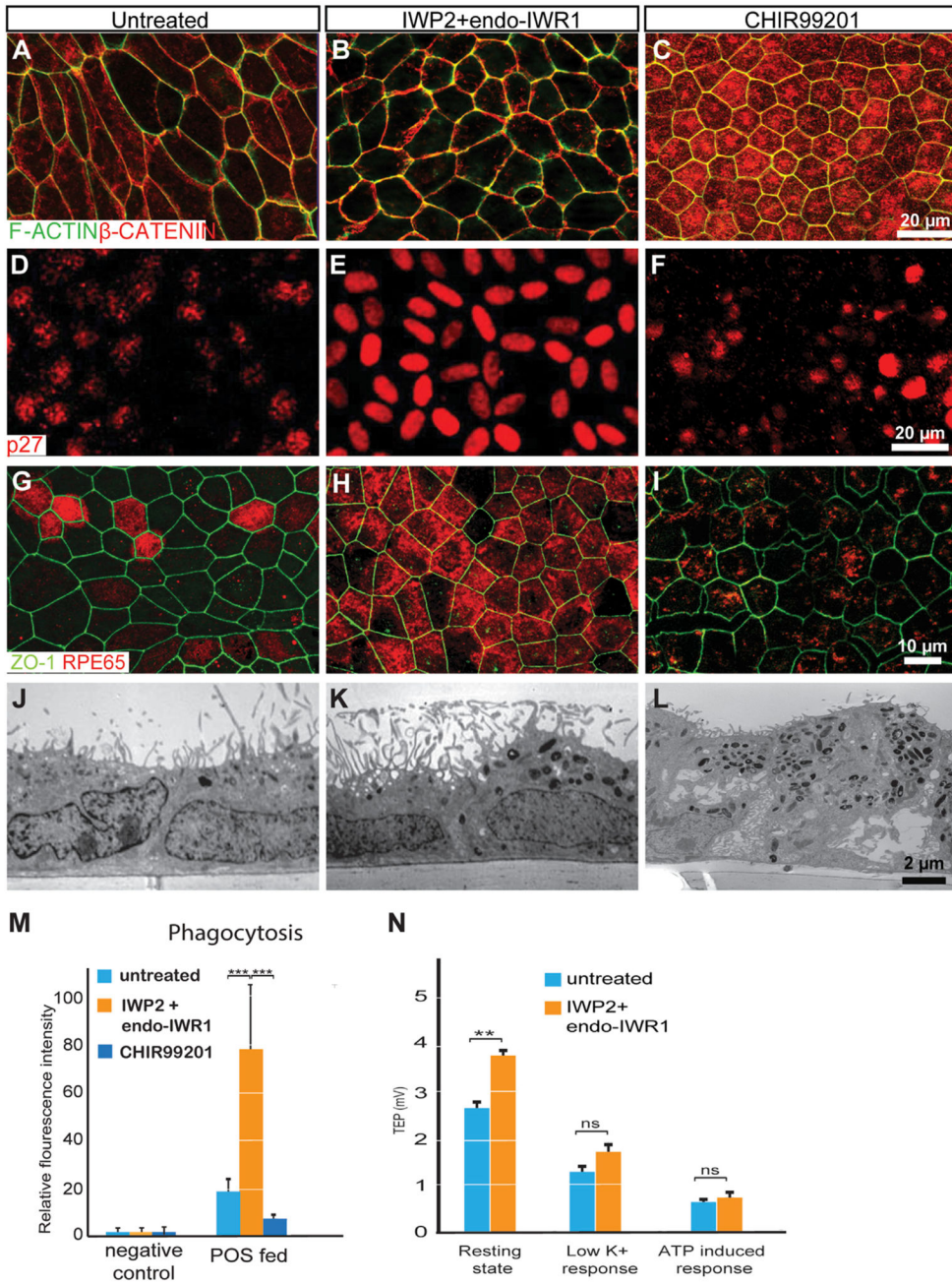


Figure 3. Canonical WNT Inhibition in iPSC-RPE Contributes to Its Maturation
 (A–L) Treatment of iPSC-RPE with the canonical WNT inhibitors IWP2 and endo-IWR1 leads to translocation of β -catenin from the cytosol to the cell membrane (B), increased expression of p27^{kip1} (E) and the RPE maturation marker RPE65 (H), and enhanced apical processes (K). In comparison treatment with the canonical WNT activator CHIR99201 causes β -catenin accumulation in the nucleus (C), low p27^{kip1} (F) and no RPE65 expression (I), and sparse apical processes (L). Similarly, untreated samples have mostly cytoplasmic β -catenin (A), low p27 (D) and RPE65 expression (G), and sparse apical processes (J).

(M) IWP2 and endo-IWR1 treatment increases the iPSC-RPE phagocytic ability 4-fold compared with untreated or CHIR99201-treated cells. *** $p < 0.001$, $n = 3$.

(N) IWP2 and endo-IWR1 co-treatment enhances the resting-state TEP of iPSC-RPE but has little effect on their electrical responses to physiological stimuli.

$n = 22$ for untreated and $n = 6$ for IWP2+endo-IWR1-treated samples; ** $p < 0.01$; ns, non-significant.

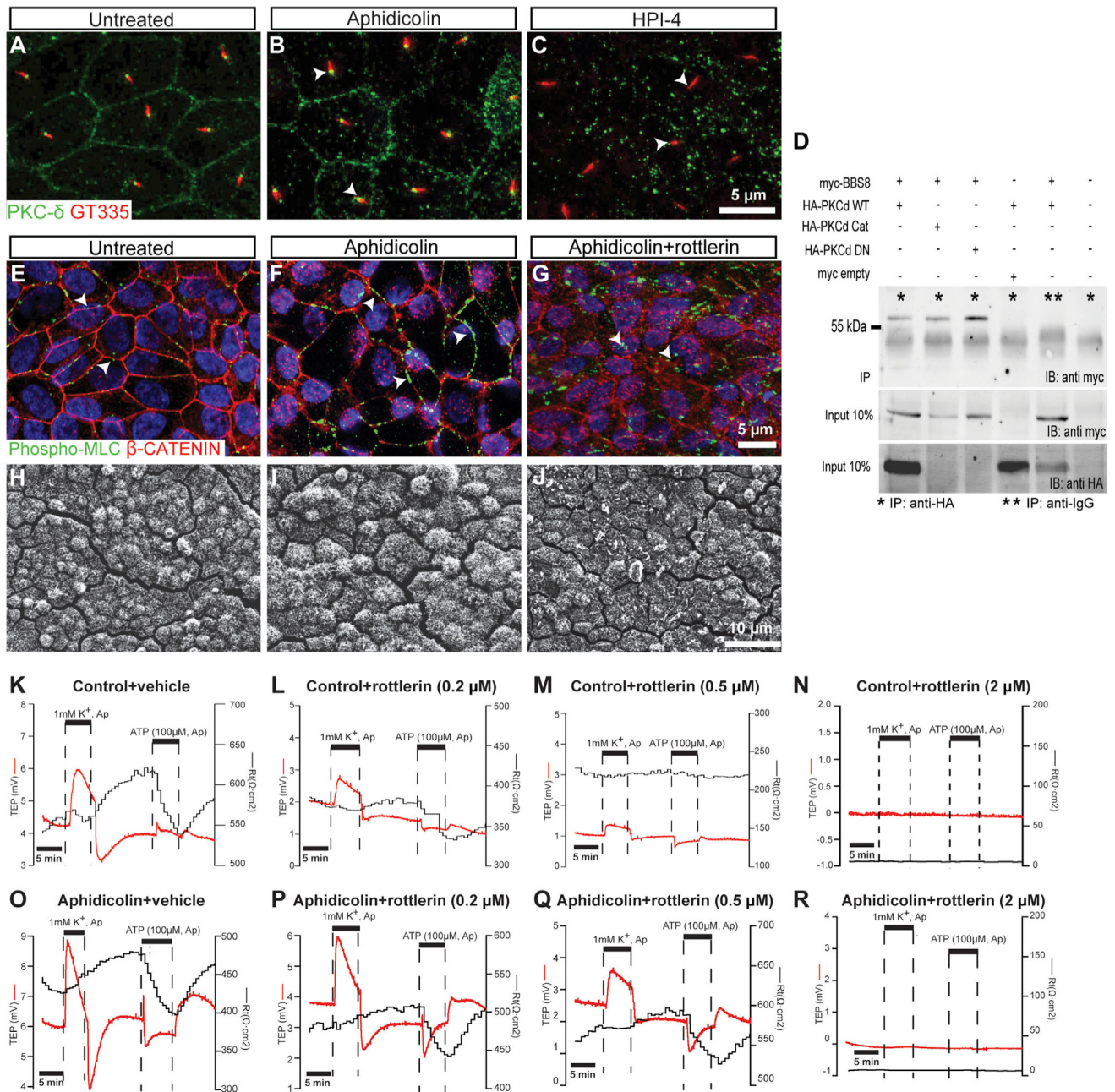


Figure 4. Primary Cilium-Induced iPSC-RPE Monolayer Maturation Is Mediated by PKCδ Activation

(A–C) Aphidicolin (B) treatment activates PKCδ (green) and causes its translocation to the base of the primary cilium as compared to HPI-4 treated (C) or untreated samples (A) (arrowheads in B and C; GT335, red). Scale bars in A–C, 5 μm.

(D) Physical interactions between BBS8-MYC and PKCδ-HA can only be detected in HEK293 cells co-expressing the two proteins. Negative controls: hemagglutinin (HA) and MYC expression plasmids and rabbit IgG. WT, catalytic domain (Cat), and dominant-negative (DN) PKCδ-HA are all able to co-immunoprecipitate with BBS8. Because of low

expression of PKC δ -HA Cat and DN, protein expression is only detectable in 100% input blots (Figure S3A).

(E–G) Phospho-Myosin Light Chain 2 (green, arrowheads), a downstream target of PKC δ , shows stronger staining along cell boundaries co-localized with β -catenin (red) in aphidicolin-treated (F) iPSC-RPE compared with untreated (E) cells or aphidicolin- and rottlerin-treated (G) samples.

(H–J) Scanning electron microscopy shows enhanced apical processes in aphidicolin-treated (I) iPSC-RPE compared with the untreated (H) control and their suppression by rottlerin treatment (J).

(K–R) Rottlerin reduces resting-state TEP/trans-epithelial resistance (TER) in a dose-dependent manner (K–N) and dampens aphidicolin-enhanced electrical responses in a dose-dependent manner (O–R) in the iPSC-RPE monolayer, suggesting a direct involvement of PKC δ in RPE monolayer maturation.

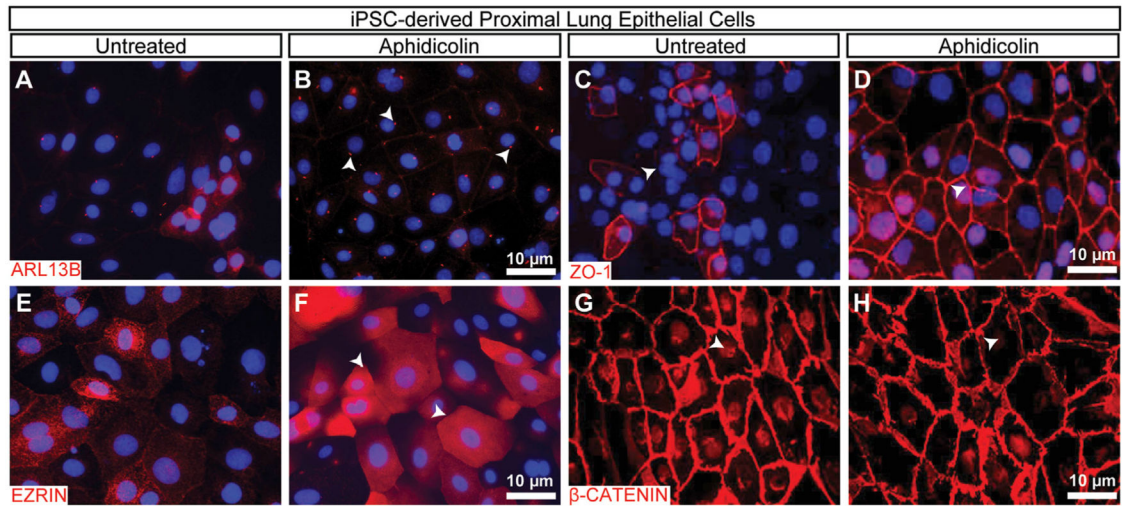


Figure 5. Experimentally Enhanced Ciliogenesis Induces hiPSC-PLEC Monolayer Maturation (A–H) Aphidicolin treatment of iPSC-PLEC during maturation enhances ciliogenesis in iPSC-PLECs (ARL13B; red, arrowheads; A and B), increases expression of the tight junction marker ZO-1 (red, arrowheads; C and D), increases expression of the polarization marker EZRIN (E and F), and facilitates β -catenin (red, arrowheads) translocation to the cell membrane (G and H).

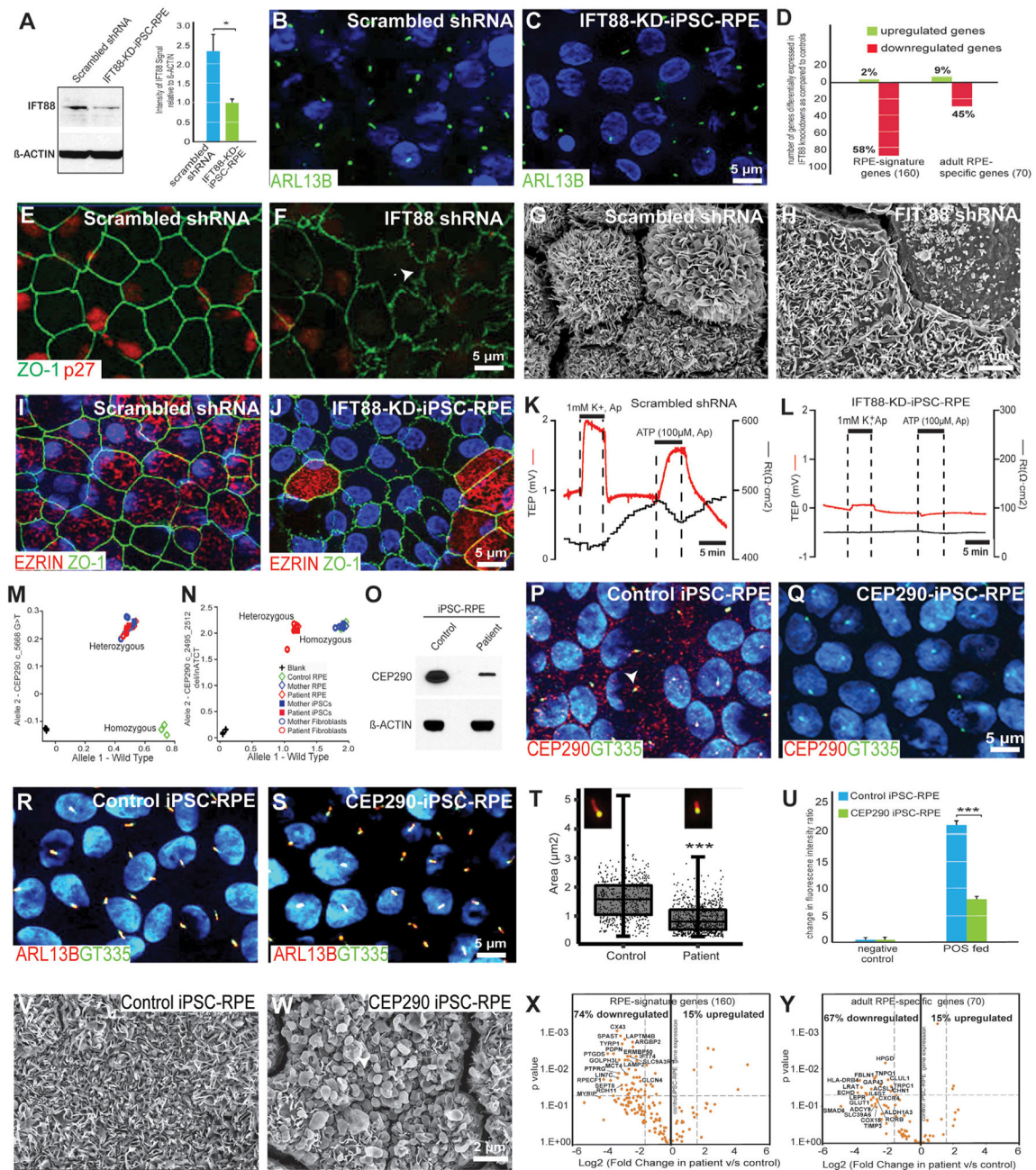


Figure 6. Defective Primary Cilia and Functional Abnormality Are Revealed in IFT88 Knockdown and CEP290-Mutated Patient-Derived iPSC-RPE

(A–L) IFT88 KD prevents primary cilium formation and compromises iPSC-RPE maturation.

(A) IFT88 protein KD in iPSC-RPE by a lentiviral IFT88 shRNA. Right: quantification of band intensity relative to b-actin; * $p < 0.05$, $n = 3$.

(B and C) Primary cilium (ARL13B, green) number is decreased in IFT88-KD-iPSC-RPE (C) compared with the scrambled shRNA control (B).

(D) 58% of RPE-signature genes and 45% of adult RPE-specific genes are downregulated in IFT88-KD-iPSC-RPE compared with the scrambled shRNA control.

(E and F) Abnormal cell morphology and dramatically decreased p27 expression in iPSC-RPE with IFT88 KD (F) compared with the scrambled shRNA control (E) (p27, red; ZO-1, green).

(G and H) Underdeveloped apical processes in iPSC-RPE with IFT88-KD (H) as compared with the control samples (G).

(I and J) IFT88-KD-iPSC-RPE (J) displays lower EZRIN expression (red) and abnormal cell morphology (ZO-1, green), as compared to scrambled shRNA control (I).

(K and L) Electrophysiological recording reveals dramatically reduced resting TEP/TER and diminished electrical responses to physiologically relevant stimuli in IFT88-KD-iPSC-RPE (L) as compared to scrambled shRNA control (K), indicating impaired RPE monolayer maturation.

(M–Y) RPE cells derived from a ciliopathy patient with Joubert syndrome show defective structural and functional maturity.

(M and N) Allele discrimination plots for CEP290 in control (green), patient (red), and patient's mother (blue) fibroblasts (circles), iPSCs (squares), and iPSC-RPE (diamonds), performed using TaqMan probes to detect (M) c.5668G > T mutation and (N) c.2495–2512 deletion. Cross, no-template control.

(O–Q) Western blot (O) and immunostaining confirms reduced CEP290 expression in patient iPSC-RPE. (P) and (Q) show GT335 (green, arrow) and CEP290 (red).

(R–T) Primary cilia in patient iPSC-RPE (S) are smaller compared with the control (R); ARL13B (red), GT335 (green). (T) shows quantification of the cilium area; two-way repeated measures ANOVA with Bonferroni correction for multiple comparisons; 5 biological repeats for both groups, *** $p < 0.001$.

(U) POS phagocytosis quantified by flow cytometry. POS phagocytic ability is 3-fold reduced in patient iPSC-RPE compared with the control; *** $p < 0.001$, $n = 3$.

(V and W) Scanning electron microscopy shows abnormal apical processes in patient iPSC-RPE (W), as compared to control samples (V).

(X and Y) Volcano plots of RPE signature (X) and adult RPE-specific (Y) genes show downregulation in the expression of 74% of RPE signature genes and 67% of adult RPE-specific genes in patient iPSC-RPE relative to the control. Genes most affected in patient samples are highlighted.

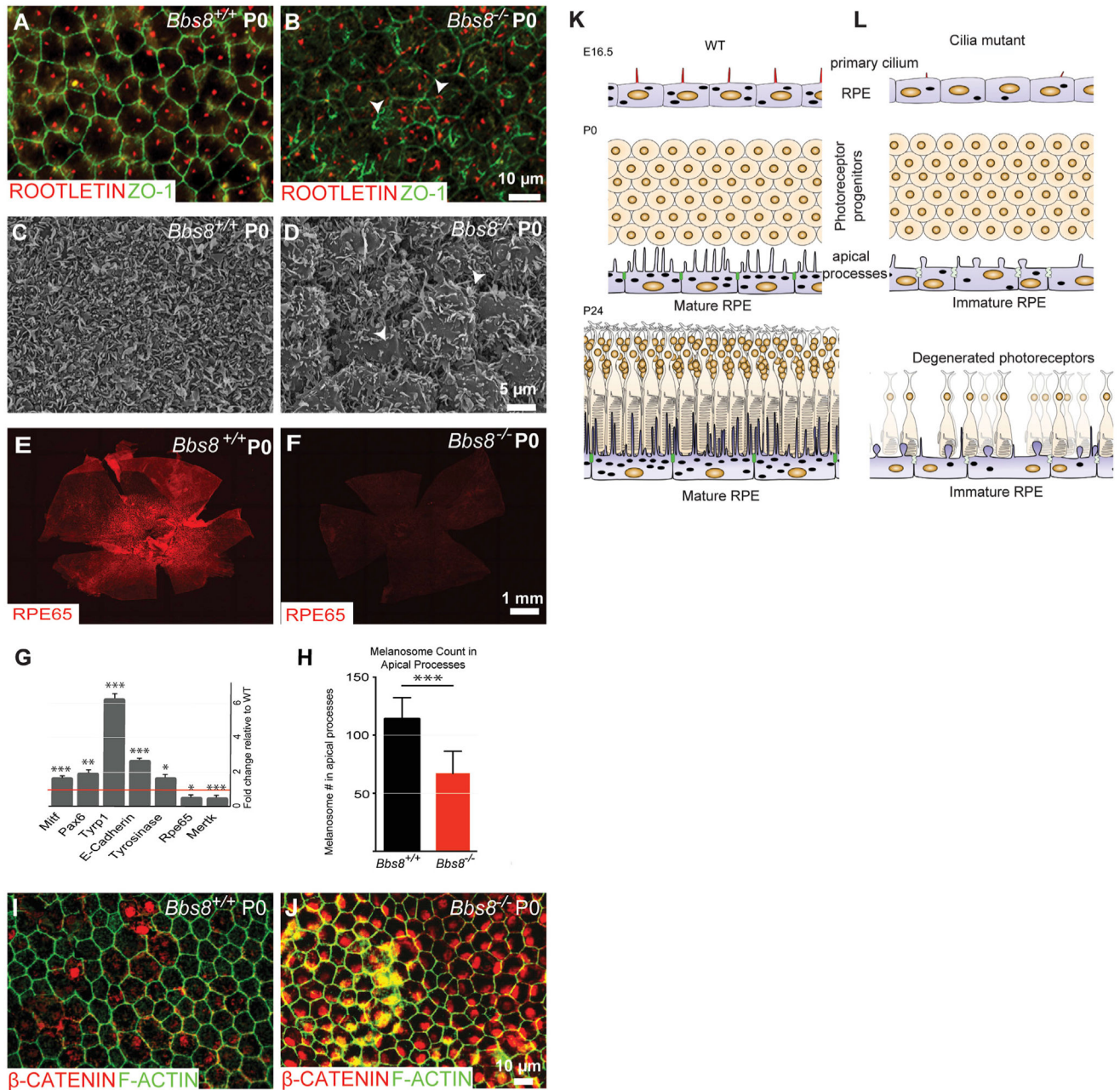


Figure 7. Defective Cilium-Induced Maturation Defects in Mouse RPE Are Mediated by Canonical WNT Overactivation
 (A and B) Disorganized ZO-1 (arrowhead, green) and ciliary rootlet (ROOTLETIN, red) staining in P0 *Bbs8*^{-/-} (B) RPE compared with the WT (A).
 (C and D) Scanning electron microscopy shows that RPE apical processes are not fully developed in *Bbs8*^{-/-} (D) mice compared with WT (C) littermates by P0.
 (E and F) In WT mouse RPE at P0, expression of the RPE maturation marker RPE65 (red) is highest near the optic nerve and decreases from the optic nerve toward the periphery (E). RPE65 expression is significantly reduced in *Bbs8*^{-/-} mouse RPE (F).

(G) qRT-PCR shows reduced expression of mature RPE markers (*Rpe65* and *Mertk*) and high expression of developmental markers (*Mitf*, *Pax6*, *Tyrp1*, *E-Cadherin*, and *Tyrosinase*) in *Bbs8*^{-/-} RPE relative to the WT (red line). *p < 0.05, **p < 0.01, ***p < 0.001; n = 5–7.

(H) Quantification of melanosome number in apical processes for WT and *Bbs8*^{-/-} mice at P16. Melanosome translocation into apical processes is reduced in *Bbs8*^{-/-} mice, suggesting underdeveloped apical processes. Two-way repeated measures ANOVA with Bonferroni correction for multiple comparisons, 4 eyes for each group.

(I and J) Nuclear β-catenin staining (red) is dramatically increased in *Bbs8*^{-/-} (J) RPE compared with WT (I) littermates (P0); F-actin is shown in green.

(K and L) Schematics summarizing our finding that dysfunctional primary cilia (L) lead to defective RPE maturation, which precedes the photoreceptor defects seen in ciliopathy mouse models(K).